Article

Macrocyclic Modalities Combining Peptide Epitopes and Natural Product Fragments

Stéphanie M. Guéret, Sasikala Thavam, Rodrigo J. Carbajo, Marco Potowski, Niklas Larsson, Göran Dahl, anita dellsén, Tom N. Grossmann, Alleyn T. Plowright, Eric Valeur, Malin Lemurell, and Herbert Waldmann

J. Am. Chem. Soc., **Just Accepted Manuscript** • DOI: 10.1021/jacs.0c00269 • Publication Date (Web): 14 Feb 2020

Macrocyclic Modalities Combining Peptide Epitopes and Natural Product Fragments

Stéphanie M. Guéret[1,2]*, Sasikala Thavam[3], Rodrigo J. Carbajo[4], Marco Potowski[3,5], Niklas Larsson[6], Göran Dahl[7], Anita Dellsén[8], Tom N. Grossmann[9], Alleyn T. Plowright[2,†], Eric Valeur[2], Malin Lemurell[2], and Herbert Waldmann[3,4]*

[1] AstraZeneca-Max Planck Institute Satellite Unit, Department of Chemical Biology, Dortmund, Germany.

[2] Medicinal Chemistry, Research and Early Development, Cardiovascular, Renal and Metabolism (CVRM), BioPharmaceuticals R&D, AstraZeneca, Gothenburg, Sweden.

[3] Max-Planck-Institute of Molecular Physiology, Department of Chemical Biology, Dortmund, Germany.

[4] Chemistry, Oncology R&D, AstraZeneca, Cambridge, United Kingdom.

[5] Faculty of Chemistry and Chemical Biology, TU Dortmund University, Dortmund, Germany.

[6] Discovery Biology, Discovery Sciences, BioPharmaceuticals R&D, AstraZeneca, Gothenburg, Sweden.

[7] Structure, Biophysics & Fragment Based Lead Generation, Discovery Sciences, BioPharmaceuticals R&D, AstraZeneca, Gothenburg, Sweden.

[8] Mechanistic Biology & Profiling, Discovery Sciences, BioPharmaceuticals R&D, AstraZeneca, Gothenburg, Sweden.

[9] VU University Amsterdam, Department of Chemistry and Pharmaceutical Sciences, Amsterdam, The Netherlands.

ABSTRACT: “Hot loop” protein segments have variable structure and conformation and contribute crucially to protein-protein interactions. We describe a new hot loop mimicking modality, termed PepNats, in which natural product (NP)-inspired structures are incorporated as conformation-determining and -restricting structural elements into macrocyclic hot loop-derived peptides. Macrocyclic PepNats representing hot loops of inducible nitric oxide synthase (iNOS) and human agouti-related protein (AGRP) were synthesized on solid support employing macrocyclization by imine formation and subsequent stereoselective 1,3-dipolar cycloaddition as key steps. PepNats derived from the iNOS DINNN hot loop and the AGRP RFF hot spot sequence yielded novel and potent ligands of the SPRY domain-containing SOCS box protein 2 (SPSB2) that binds to iNOS, and selective ligands for AGRP-binding melanocortin (MC) receptors. NP-inspired fragment absolute configuration determines the conformation of the peptide part responsible for binding. These results demonstrate that combination of NP-inspired scaffolds with peptidic epitopes enables identification of novel hot loop mimics with conformationally constrained and biologically relevant structure.

▪INTRODUCTION

For small molecule modulation of protein-protein interactions (PPIs) mediated by extended binding surfaces,[1] new approaches and chemical modalities are in high demand.[2,3] Recently, loop segments composed of peptide sequences displaying diverse structures and with their termini positioned in spatial proximity ("Ω loops") were identified as frequently occurring protein structural motifs, mediating numerous PPIs ("hot loops").[4,5]

For inhibition of PPIs mediated *via* hot loops, macrocyclic peptides have been increasingly explored in recent years,[6,7,8] and, in particular, disulfide bridges[9,10,11], aromatic thioethers[12] and alkyne linkers[13] were established to connect amino acid side chains in peptides.[14] Mixed macrocycles have been reported to decorate peptide sequences with aziridines,[15] iminoborane phenyl units,[7] oxadiazoles,[16] heteroaryl scaffolds[17,18] and aromatic moieties.[7,8,16,19,20] In addition, in individual cases hybrid macrocycles which incorporate sp^3-configured stereocenters inspired by natural product (NP) structure have recently been reported with the cyclization in general performed in solution after solid phase peptide synthesis (SPPS) of precursors.[21,22] Notably, flexible modification of the peptide moiety in the rapamycin macrocycle led to

potent, isoform-specific and FKBP-dependent inhibitors of the equilibrate nucleoside transporter, an activity that differs from the original Rapamycin target, FK506-binding protein.[23] New methods that give rapid and versatile synthetic access to such macrocycles would offer novel opportunities to the modulation and study of challenging PPIs and expand the tool box of available hybrid macrocycle.

Hot loops can adopt diverse conformations such that application of established techniques and small molecule classes for PPI modulator design is complicated or even impeded.[24] Thus, macrocycles are in high demand, in which the peptide conformation can efficiently be installed or adjusted through non-peptidic units which themselves may primarily modulate but not directly mediate binding.

Macrocycles combining peptidic and chiral non-peptidic structural elements, such as polyketide (e. g. the chondramides/jasplakinolides[25]) or biaryl[26] motifs (e.g. the biphenomycins[27] and arylomycins[28]), potently modulate PPIs. In these hybrid NPs, the stereogenic character of both the amino acids and the non-peptidic units determines the overall conformation.[29, 30, 31] For example, in the case of the chondramides, the polyketide unit may point away from the binding surface of their target, actin. Nevertheless, modifications in the stereochemistry of the polyketide region force the

macrocycle in a conformational manifold that leads to differing binding.[25] This finding suggests that hot loop mimics with adjustable conformation could be developed by combination of peptidic epitopes derived from relevant "Ω loops" with chiral non-peptidic units linking their *C*- and *N*-termini. Structure and configuration of these stereogenic NP-inspired elements should be efficiently adjustable through asymmetric synthesis.

Beyond macrocyclic natural product-inspired hybrids, PPI modulators are frequently derived from chiral natural products (NPs),[32] and cheminformatic analysis indicates that the properties of these NPs are conserved in and represented by NP-inspired fragments and scaffolds, including stereogenic character.[33] Therefore, we envisioned combining NP-inspired structures with peptide sequences from hot loops to yield macrocyclic **Pep**tide-**Nat**ural product-inspired hybrids ("**PepNats**") as a novel modality to modulate PPIs (Figure 1). For efficient access to PepNats, both peptide and stereoselective NP synthesis should ideally be carried out on solid support. However, complexity and diversity generating transformations for NP-inspired scaffold synthesis on solid support have been explored only for selected structures.[34, 35, 36, 37, 38]

Successful combination of both stereoselective NP-inspired scaffold synthesis and peptide synthesis was only reported in few cases and in solution.[21 , 39 , 40]

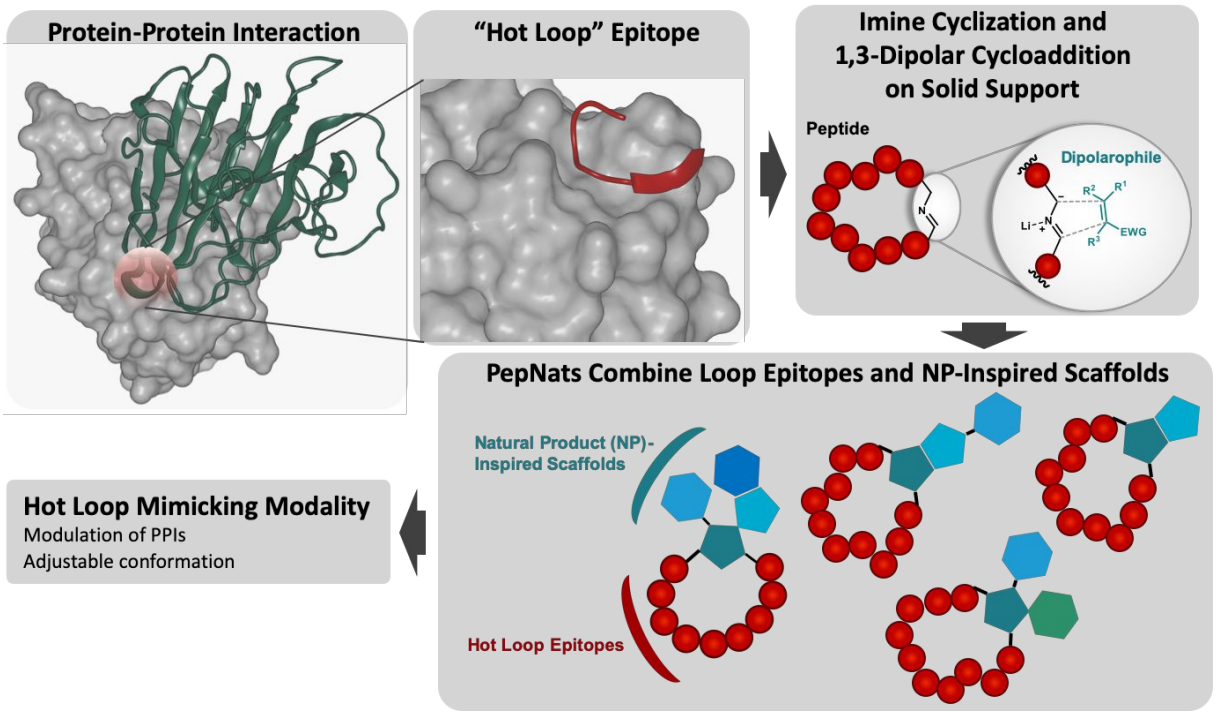

Figure 1. Strategy for the development of **Pep**tide-**Nat**ural product-inspired hybrids (**PepNats**). The structure of the protein-protein interaction and the "hot loop" epitope are derived from the crystal structure with PDB 3EMW. The amino acids of the peptide sequence of interest are represented by red balls and the natural product-inspired scaffolds are depicted in blue and green.

Herein, we report the design, synthesis and biological investigation of structurally diverse macrocyclic PepNat collections mimicking hot loop epitopes. Peptide synthesis

on solid support followed by macrocyclization *via* imine formation enabled subsequent pyrrolidine ring formation by means of stereoselective 1,3-dipolar cycloaddition on resin. Investigation of the PepNats for hot loop mimicry of inducible nitric oxide synthase (iNOS) and of the human agouti-related protein (AGRP), yielded novel potent ligands for the SPRY domain-containing SOCS (suppressor of cytokine signaling) box protein 2 (SPSB2) and selective ligands and agonists for the melanocortin (MC) receptors respectively.

▪RESULTS AND DISCUSSION

Solid phase synthesis strategy

To establish a flexible synthesis, we envisioned a stereoselective 1,3-dipolar cycloaddition reaction of azomethine ylides on solid support as the key step. The azomethine ylides would be generated *in situ* on resin by deprotonation of appropriately functionalized cyclic peptide imines, obtained by macrocyclization of linear peptides through Schiff base formation (Figure 1). This cycloaddition reaction has previously been employed for the highly stereoselective solution-[41, 42, 43] and solid-phase[44, 45, 46] synthesis of different NP-inspired scaffolds containing multiple stereogenic centers. It provides efficient and flexible access to fused- and spiro-pyrrolidine NP-inspired structures from a common azomethine ylide by variation of the dipolarophile with simultaneous establishment of up to four stereocenters. Recently, imine formation followed by reductive amination has been employed before for peptide cyclization in solution.[39]

Initially, a test peptide sequence (ALFPGF) **2** was assembled on commercially available Rink Amide low loading resin and equipped with a glycine and a N-methyl phenylalanine (Scheme 1, aa^2 = Phe) dipeptide at the *N*-terminus as well as a 4-

methyltrityl (Mtt)-protected lysine at the *C*-terminus. After Mtt deprotection, an aromatic aldehyde was installed at the lysine side chain to afford peptide **3**. Following the removal of the Fmoc protecting group, a one pot sequence was developed on resin, which consists of intramolecular cyclization through Schiff base **4** formation using trimethyl orthoformate as the dehydrating agent (for imine formation screening conditions, see Supplementary Table S1), azomethine ylide generation and 1,3-dipolar cycloaddition. In the presence of lithium bromide, different dipolarophiles **6**, **7**, **10**, **11** (Figure 2) were quantitatively converted to the desired cycloadducts (Supplementary Table S2, entries 8–11). After release from the resin, removal of side chain protecting groups and purification by reverse phase chromatography, the major diastereomer of the desired cycloadducts **A1**–**A4** was obtained in overall yields of 8 to 14 % from the starting unfunctionalized Rink Amide resin, through a total of six steps after the SPPS linear precursor synthesis on resin (Supplementary Table S3, entries 1–4).

Scheme 1. Synthesis of macrocyclic PepNats using the imine/cycloaddition strategy on solid support.

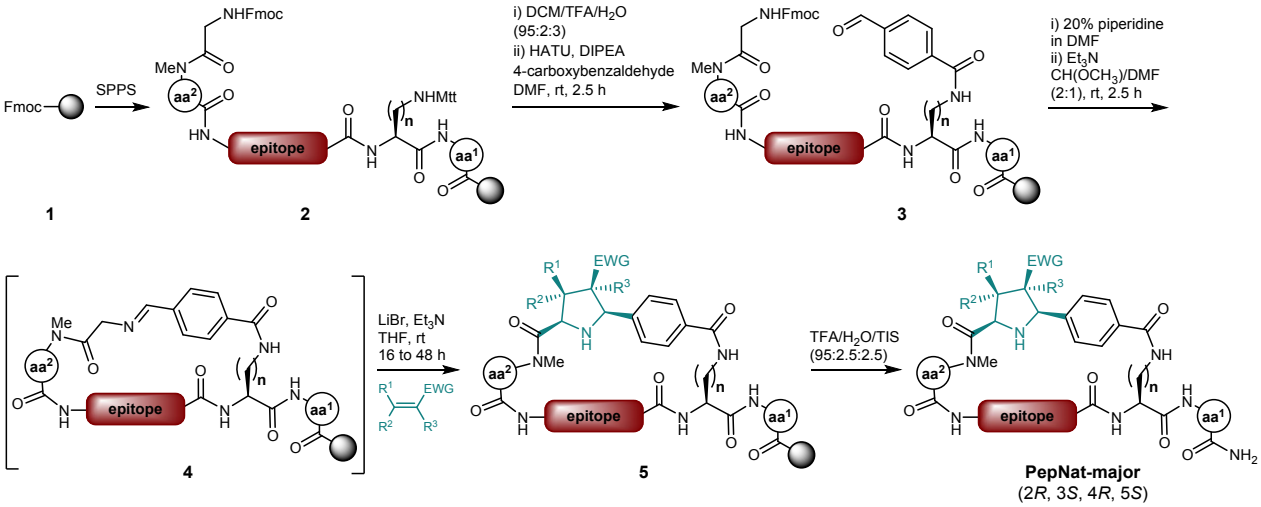

1 = Rink Amide resin (loading = 0.16 to 0.36 g.mol^{-1}); SPPS = Solid Phase Peptide Synthesis; epitope = peptide sequence inspired from hot loop epitope (for complete list of peptide epitope see Supplementary Table S3); n = 1 to 4 carbon linker length; aa = amino acid (for details see Figure 3, 4 and Supplementary Table S3 and S4); R^1, R^2, R^3 and EWG (Electron Withdrawing Group) are a schematic representation of the dipolarophiles (Figure 2).

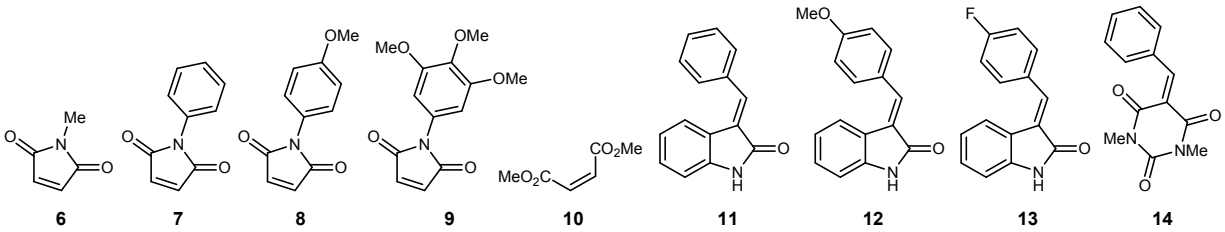

Figure 2. Structure of dipolarophiles (**6**–**14**) used in the 1,3-dipolar cycloaddition on solid support.

The influence of resin loading on the different steps of the synthesis was investigated using commercially available Rink Amide low loading resin (loading 0.26 to 0.36 mmol.g^{-1}) (Figure 3a, Table entries 1, 3, 5, 7, 8, 9, 10 and 12). In addition, lower loaded starting Rink Amide resin (loading = 0.19 to 0.16 mmol.g^{-1}) was obtained by capping the resin with acetylated glycine (Figure 3a, Table entries 2, 4, 6, 11). The resin loading

and related conversions during the SPPS and the aldehyde coupling (Figure 3a) were determined by treatment of the Fmoc-protected related resin with 20% piperidine in DMF followed by quantification by UV-Vis spectroscopy of the dibenzofulvene-piperidine adduct at 301 nm maximum absorbance wavelength and 8021 $l.mol^{-1}.com^{-1}$ molar absorption coefficient using Lambert-Beer's law for calculation (for details see Supplementary Information, Section 3a). Overall, the SPPS of the linear peptide precursors proceeded with ca. 50 to 60% conversion. Lower loading resin allowed a slightly better synthesis efficiency of the desired linear precursor by SPPS (Figure 3a, compare entries 2 and 1 with entries 11 and 10 respectively). After Mtt cleavage, the coupling of the aromatic aldehyde to the unprotected lysine residue of the various linear precursors proceeded with viable conversions from 64 to 94%. According to the experimental loading of the functionalized aldehyde peptide precursor on resin, the yield of the imine cyclization followed by cycloaddition was determined for the isolated major diastereomers after purification by reverse phase chromatography. The use of low functionalized resin did not improve the isolated yield for the imine/cycloaddition final step to access the PepNats. For the longer and less demanding peptide sequences (GNMeFALFPGFG and GNMeFDINNNKG Figure 3a, entries 1–6), the

cycloaddition using maleimide dipolarophiles, **6** and **8** proceeded with viable isolated yields (ca. 20% yield), independent of the initial loading of the starting resin. Lower isolated yields for the cycloaddition step were observed when hindered dipolarophile **14** (Figure 3a, entry 7) or hindered peptide sequences such as RffN and Rff (Figure 3a, entries 8–12) were used. In these cases, the use of lower loading resin did not improve the isolated yield of the major diastereomer after imine formation and cycloaddition. In accordance with these observations and to allow rapid access to various PepNats and modifications, the commercially available Rink Amide low loading resin was used without further modification. Yields are reported as overall isolated yields for the major diastereomers after reverse phase chromatography from the starting resin.

a

entry	Resin loading (g.mol^{-1})	Peptide sequence†	SPPS loading (g.mol^{-1})	SPPS conv. (%)	Aldehyde coupling loading (g.mol^{-1})	Aldehyde coupling conv. (%)	Imine cyclization/Cycloaddition dipolarophile	d.r.‡	PepNat major	isolated yield (%)	overall yield (%)§
1	0.36	G-NMeF-ALFPGFKG	0.18	49	0.12	67	**6**	92:8	**A1**	22	8
2	0.19	G-NMeF-ALFPGFKG	0.15	76	0.10	68	**6**	92:8	**A1**	13	6
3	0.26	G-NMeF-DINNNKG	0.17	65	0.16	94	**6**	96:4	**D1**	24	11
4	0.18	G-NMeF-DINNNKG	0.12	64	0.09	79	**6**	96:4	**D1**	21	5
5	0.26	G-NMeF-DINNNKG	0.17	64	0.15	88	**8**	81:19	**D3**	20	10
6	0.18	G-NMeF-DINNNKG	0.12	67	0.09	79	**8**	84:16	**D3**	23	6
7	0.34	G-NMeF-DINNNKG	0.14	41	0.09	64	**14**	71:29	**D7**	11	4
8	0.34	G-NMeV-DINNNKG	0.18	54	0.13	71	**7**	62:38	**D18**	4	2
9	0.36	G-NMeV-INNNKG	0.17	47	0.14	82	**7**	58:42	**D22**	7	3
10	0.34	G-NMeF-RffNKG	0.19	56	0.14	75	**6**	51:49	**K2***	3	1
11	0.16	G-NMeF-RffNKG	0.11	69	0.09	82	**6**	50:50	**K2***	3	2
12	0.26	G-NMeF-RffKY	0.04	16	0.03	75	**6**	61:39	**O1**	7	1

b

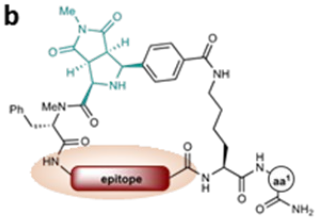

PepNat	ring size	epitope†	aa¹	conv. (%)	d.r.‡	yield (%)§	purity (%)#
D19-major	12	EEKDINNNVKT		≥ 99	70:30	2	91
D20-major	8	DINNNV	G	≥ 99	84:16	5	99
D1-major	7	DINNN	G	≥ 99	96:4	11	96
D21-major	6	INNN	G	≥ 99	66:34	3	74
D23-major	5	NNN	G	≥ 99	75:25	12	98

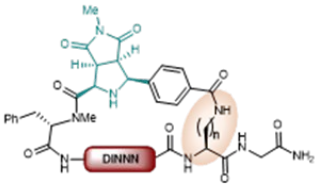

PepNat	n	conv. (%)	d.r.‡	yield (%)§	purity (%)#
D1-major	4	≥ 99	96:4	11	96
D8-major	3	≥ 99	96:4	13	97
D9-major	2	≥ 99	95:5	3	97
D10-major	1	≥ 99	84:16	4	98

c

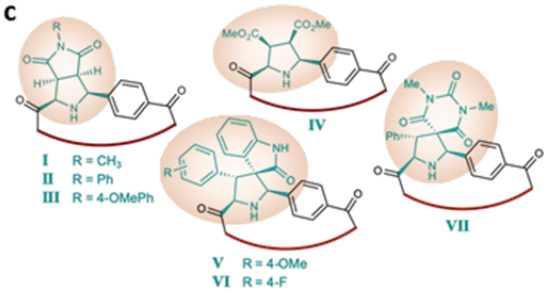

PepNat	dipolarophile	NP unit	conv. (%)	d.r.‡	yield (%)§	purity (%)#
D1-major	6	I	≥ 99	96:4	11	96
D2-major	7	II	≥ 99	83:17	5	83
D3-major	8	III	≥ 99	81:19	10	93
D4-major	10	IV	≥ 99	59:41	6	85
D5-mixt	12	V	≥ 99	11:10:17:62	3	96
D6-major	13	VI	≥ 99	9:36:7:48	6	89
D7-major	14	VII	≥ 99	71:29	4	88

d

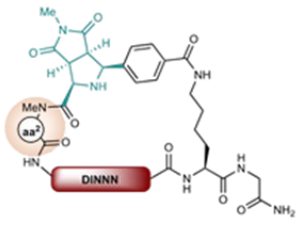

PepNat	NMe-aa²	conv. (%)	d.r.‡	yield (%)§	purity (%)#
D1	NMeF	≥ 99	96:4	11	96
D11	NMeG	≥ 99	54:46	8	90
D12	NMeL	≥ 99	91:9	10	95
D13	NMeV	≥ 99	85:15	11	98
D14	P	≥ 99	57:43	3	94
D15	NMef	≥ 99	64:36	5	97
D16	F	≥ 99	28:35:37	2	81

Figure 3. Scope of the imine/cycloaddition on solid support. † Depicted as single capital letter code; D-amino acids are indicated by lower case letter. ‡ Depicted as major:minor isomers unless more than two diastereomers were obtained; d.r. determined from the crude product by integration of the analytical- or

optimized-RP-HPLC-MS profile at 210 nm (for details see the Supplementary Information). § Overall isolated yield after preparative-RP-HPLC calculated from the loading of the starting unfunctionalized rink amide resin. # Purity of isolated PepNats determined by integration of the product peak of the HPLC profile (210 nm). conv. conversion was determined by integration of the product and starting material (SM) peaks using the analytical RP-HPLC profile at 210 nm. * reverse diastereoselectivity observed (for details see Supporting Information). (a) Impact of the starting resin loading for each step of the strategy (SPPS, Mtt cleavage/aldehyde coupling and imine cyclization/cycloaddition reaction). The loading was quantified by the UV absorbance of the piperidine-dibenzofulvene adduct after Fmoc deprotection of the functionalized resin (for details see the Supplementary Information). (b) Ring size accessibility by variation of the epitope length and carbon linker of the lysine unit. (c) Scope of the dipolarophiles (for structures see Figure 2) used for the cycloaddition on resin. (d) Variation of N-methylated amino-acid α to the natural product-inspired unit.

For the DINNN epitope peptide sequence, the synthesis proved robust and of wide scope (Figure 3b–d). The length of the amino acid sequence flanking the DINNN epitope was successfully varied from nine to three amino acids (Figure 3b, top table). Further structural variation was achieved by shortening the side chain of the amino acid employed for aldehyde attachment to afford PepNats **D1**, **D8**–**D10** with viable diastereoselectivity (Figure 3b, bottom table). Seven different PepNats bearing the unique DINNN peptide sequence epitope were obtained by variation of the dipolarophile used in the cycloaddition (Figure 3c). Moreover, the impact of an N-

methylated amino acid (aa^2) was investigated (Figure 3d). The stereoselectivity of the cycloaddition increased with the size of the N-methylated amino acid next to the glycine employed for imine formation (e.g. compare **D1** with **D11**) and N-alkylation was beneficial (compare **D1** with **D14** and **D16**). A wide range of aa^2 was tolerated including an N-methylated β-branched amino acid (PepNat **D13**).

Variation of amino acid structure (polar, hydrophobic and β-branched) and peptide epitope sequences (two to nine amino acids) as well as the dipolarophile (**6**–**14**, Figure 2) yielded a diverse collection of 63 macrocyclic PepNats typically in multimilligram amounts and with excellent purity (Figure 4, Supplementary Table S3 and S4). In total 16 different peptide loop epitope sequences mainly derived from PPIs[5] were obtained by the solid-support synthesis methodology to yield a wide range of ring sizes (3 to 12 amino acids).

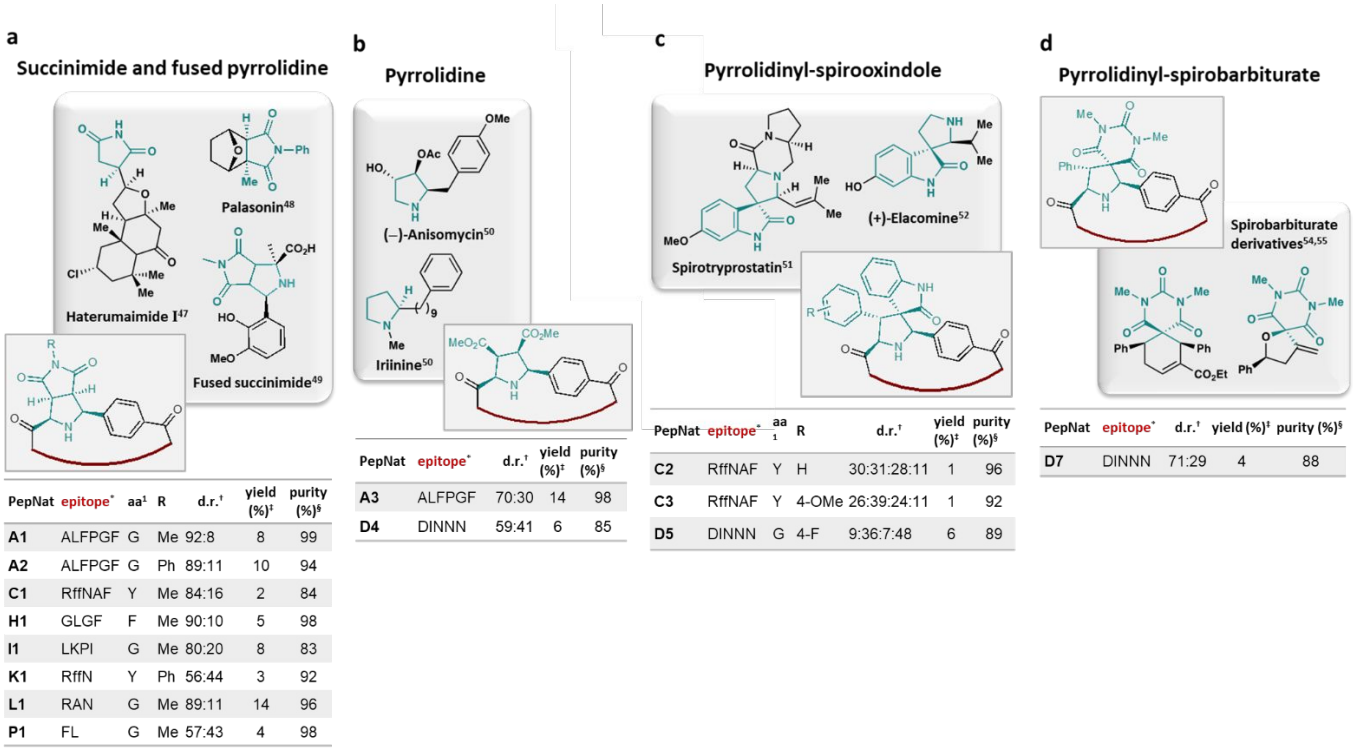

PepNat	epitope*	aa[1]	R	d.r.†	yield (%)‡	purity (%)§
A1	ALFPGF	G	Me	92:8	8	99
A2	ALFPGF	G	Ph	89:11	10	94
C1	RffNAF	Y	Me	84:16	2	84
H1	GLGF	F	Me	90:10	5	98
I1	LKPI	G	Me	80:20	8	83
K1	RffN	Y	Ph	56:44	3	92
L1	RAN	G	Me	89:11	14	96
P1	FL	G	Me	57:43	4	98

PepNat	epitope*	d.r.†	yield (%)‡	purity (%)§
A3	ALFPGF	70:30	14	98
D4	DINNN	59:41	6	85

PepNat	epitope*	aa[1]	R	d.r.†	yield (%)‡	purity (%)§
C2	RffNAF	Y	H	30:31:28:11	1	96
C3	RffNAF	Y	4-OMe	26:39:24:11	1	92
D5	DINNN	G	4-F	9:36:7:48	6	89

PepNat	epitope*	d.r.†	yield (%)‡	purity (%)§
D7	DINNN	71:29	4	88

Figure 4. Top: Representation of Natural Product (NP)-inspired scaffolds contained in the PepNats. Bottom: Illustrative examples of PepNats (major diastereomer) obtained through the imine/cycloaddition synthesis on solid support. Selected examples (for a complete list see Supplementary Tables S3 and S4). * Depicted as single capital letter code with D-amino acids indicated by lower case letter. † Depicted as major:minor isomers unless more than two diastereomers were obtained; d.r. determined from the crude product by integration of the analytical- or optimized-RP-HPLC-MS profile at 210 nm (for details see Supplementary Information). ‡ Overall isolated yield after preparative-RP-HPLC from the starting unfunctionalized resin. § Purity of isolated PepNats determined by integration of the product peak of the HPLC profile (210 nm). (a) Selected examples of NPs bearing succinimides and fused succinimide-pyrrolidines. These NPs inspired the structure of the fused di-pyrrolidine PepNats obtained through the cycloaddition in the presence of maleimide dipolarophiles **6**–**9** (for structures see Figure 2). (b) Selected examples of pyrrolidine NPs which inspired the synthesis of the pyrrolidine-peptide macrocyclic PepNats. (c) Selected examples of spirooxindole containing NPs and related representative structure of the 3,3'-pyrrolidinyl-spirooxindole inspired PepNats obtained through the cycloaddition in the

presence of arylidene oxindoles **11**–**13** (for structures see Figure 2). (d) Representative structure of the pyrrolidinyl-spirobarbiturate containing PepNat and selected example of spirobarbiturate derivatives.

Using a variety of peptide epitopes inspired by hot loops, the NP-inspired unit of the PepNats was readily changed by variation of the dipolarophiles used in the 1,3-dipolar cycloaddition after intramolecular imine formation on resin (Figure 3c and 4). The maleimide dipolarophiles **6**–**9** afforded fused di-pyrrolidine-peptide macrocycles (e.g. **A1–2**, **C1**, **H1**, **I1, L1, K1, P1**, Figure 4a) which embody the heterocyclic scaffold characteristic of NPs bearing succinimides[47, 48] and fused succinimide-pyrrolidine analogues[49] (Figure 4a), whereas use of dimethyl maleate **10** led to incorporation of pyrrolidines (e.g. **A3**, **D4**, Figure 4b) into the hybrid macrocycle, reminiscent of the underlying scaffolds of pyrrolidine alkaloids.[50] The arylidene oxindoles **11**–**13** delivered PepNats (e.g. **C2**, **C3**, **D6**, Figure 4c) combining a macrocyclic peptide structure and a 3,3'-pyrrolidinyl-spirooxindole scaffold, inspired by the naturally occurring spirooxindole alkaloids and pyrrolidine fused spirooxindole.[51, 52, 53]

Barbiturate-derived alkene dipolarophile **14** introduced additional diversity through incorporation of the pyrrolidinyl-spirobarbiturate scaffold (Figure 4d)[54, 55, 56] in the PepNat (e.g. **D7**, Figure 4d).

With LiBr as catalyst, the 1,3-dipolar cycloaddition in the presence of *N*-substituted maleimides typically yielded two *endo* cycloadducts in stereoisomer ratios of 51:49 to 96:4, which could not be increased by using chiral Cu- or Ag-Fesulphos catalysts,[57] indicating that the transformation is substrate-controlled. For arylidene-oxindoles, four diastereomers were formed, probably due to *E*/*Z*-isomerization of the dipolarophiles or ring opening/closure of the cycloadduct.[58]

For assignment of absolute configuration, enantiopure (2*S*, 3*R*, 4*S*, 5*R*)-configured cycloadducts derived from *N*-Me- and *N*-Ph-maleimide dipolarophiles were synthesized independently in solution, employing the chiral Cu-*R*-Fesulphos catalyst complex and converted to diastereomerically pure PepNats **H1-minor**, **K1-minor**, **D9-minor** and **D10-minor**, embodying GLGF-, RffN- and DINNN-epitope sequences respectively (for synthesis of **H1-minor** and **K1-minor** see Supplementary Figure S1; for choice of the epitope sequences, see below). Comparison of NMR spectra and HPLC retention times revealed that in all cases, the (2*R*, 3*S*, 4*R*, 5*S*) diastereomer was formed in excess (Supplementary Figures S2 and S3). Therefore, the 1,3-dipolar cycloaddition on resin, by analogy to the solution reaction, proceeds *via* an *endo*-transition state, steered here by the peptide moiety. Macrocyclic peptides and

peptidomimetics adopt in general relatively rigid conformations,[24, 59, 60] which here would lead to formation of *E*-configured ω-shaped azomethine ylides embedded in the macrocycles. The dipolarophiles would then approach from the less hindered *si* face of the dipole (Supplementary Figure S4). The configurations of the pyrrolidinyl spirooxindole and spirobarbiturate cycloadducts were assigned by analogy.

Conformational analysis

Analysis of the NMR spectra of the major (2*R*, 3*S*, 4*R*, 5*S*)-diastereomer of PepNats **H1-major** and **K1-major** (Supplementary Information, Section 5) revealed that these macrocyclic peptide hybrids adopt very different conformations in solution. Introduction of a stereogenic NP-inspired fragment appears to lock the cyclic loop mimics into relatively stable conformations, which should favor defined molecular interactions with target proteins.

To determine the structure of the conformers present in solution, the conformational space for each peptide was thoroughly explored using the Maestro Macrocycle Sampling algorithm (OPLS3 force field; version 11.6.013, Schrödinger) with an energy threshold of 25 Kcal/mol to allow for a full exploration of the rotation around the peptidic

bonds. First, the resulting conformers were filtered to a reduced set of conformations that matched key long-range nOes in the macrocycle. To avoid being too restrictive and missing possible conformers complying with the NMR data, the filter for those distances was set to an upper limit of 5.5 Å. Each of the conformers from the reduced set was subjected to solvent explicit 10 ns MD simulations that were subsequently clustered by RMSD. The most populated cluster for each conformer was taken as the conformation which the molecule adopted most time in the dynamics run.[61] The average structure for each of the most populated clusters was extracted and a new reduced set of conformations comprising each of the averaged structures was used together with the experimental NMR restraints (nOes and *J* couplings) to find the best fit via MSpin's least squares algorithm (MSpin nOe Fitter algorithm, version 2.4.0-713; MestReLab Research). Intramolecular H-bond information from sample exchange in CD_3OD was used for further refinement and introduced as distance restraints. The clusters and the corresponding averaged structures for macrocycles **H1-major** and **H1-minor** that showed the best agreement with the experimental NMR data are shown in Figure 5. In addition, to the nOes and the intramolecular H-bonds, an extra indication that the macrocycles are structured derives from the $^{3}J_{\text{NH-H}\alpha}$ values found for the backbone

amides. Four of the amides in **H1-major** and three in **H1-minor** out of a total of six show couplings deviating from the 7.5 Hz mean, the value normally interpreted as arising from free mobility (see Supporting Information).[62]

Notably, key NMR information shows major differences in the conformational space explored by **H1-major** and **H1-minor**. For example, the fused di-pyrrolidine *N*-methyl group in the major PepNat **H1-major** isomer embodying the GLGF sequence displayed long-range nOe interactions with the peptide backbone (Supplementary Figure S5), whereas only minor interactions in the form of long-range nOes with the leucine side chain were detected for the minor isomer **H1-minor** (Supplementary Figure S6). In the conformation of the major isomer, the *N*-methyl group of the NP points towards the macrocycle peptidic core and comes close to the glycine and phenylalanine in the transannular position (Figure 5, left). In the minor diastereomer, the *N*-methyl group does not face the peptide backbone but is instead in proximity to the leucine (Figure 5, right).

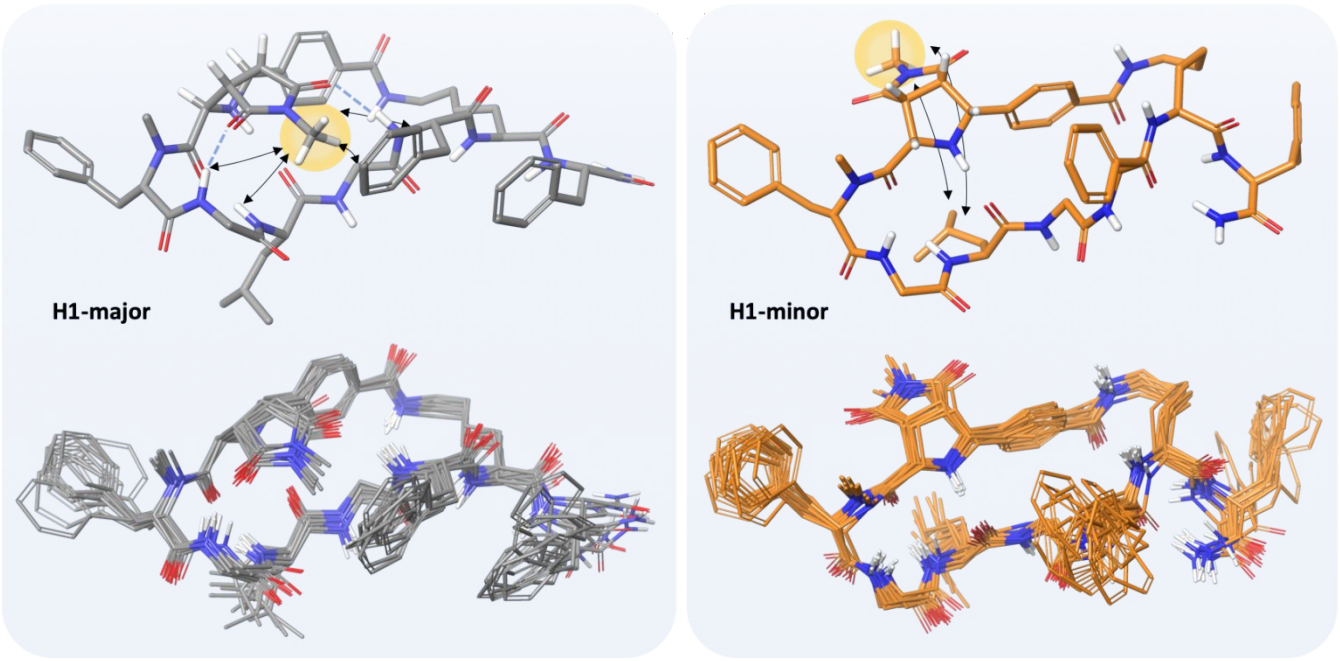

Figure 5. NMR derived best-fit cluster and average structure for the fused di-pyrrolidine PepNat **H1** major and minor diastereomers. Arrows indicate key long-range NMR nOe interactions with the *N*-methyl group of the fused di-pyrrolidine unit. Additional long range nOe interactions were observed between other regions of the peptides but are not shown for clarity. Dashed blue lines indicate intramolecular hydrogen bonds observed in the NMR data between the peptide backbone and C=O groups of the fused di-pyrrolidine unit.

NMR analysis of the PepNat **K1-minor** obtained through on resin cycloaddition between the *N*-phenyl maleimide and the Schiff base incorporating the RffN epitope revealed long range nOe cross peaks between the *N*-phenyl substituent of the fused di-pyrrolidine unit and the Rff motif. In the case of **K1-minor**, the increased number of aromatic rings in the molecule led to a large overlap of the NMR signals and an excess of ambiguous nOe restraints that precluded a full conformational analysis of the

structure (Supplementary Figure S7 and Supplementary Information, Section 6). Similarly, the highly complex NMR spectra of **K1-major** prevented a full assignment of the structure.

These results indicate that the PepNat hot loop mimic collection is not only structurally and stereochemically diverse, but also conformationally diverse. The different defined solution conformations should enable tunable interactions with target proteins. Indeed, the major and minor isomers displayed very different bioactivity (see below).

DINNN-PepNats bind to the SPSB2 protein

Hot loop mimicry was investigated using the iNOS–SPSB2 protein-protein interaction as a representative example. iNOS produces nitric oxide and plays key roles in the immune system and defense against infections.[63] SPSB2 is the adaptor protein in the E3 ubiquitin ligase complex that ubiquitinates iNOS, targets it for proteasomal degradation and therefore modulates its lifespan. The conserved DINNN type II β-turn loop motif of the *N*-terminal region of iNOS is the key binding epitope for the SPSB2 protein,[63, 64, 65] and has been classified as a "hot loop".[5] Disulfide-, lactam-bridged and simple aromatic non peptidic scaffolds have been employed to close the DINNN epitope and led to cyclic peptides and peptidomimetics that confirm the importance of

this loop for the iNOS–SPSB2 interaction.[7, 11, 66] Flexible incorporation of adjustable NP-inspired scaffolds to close the DINNN motif has not yet been reported and would readily give access to multiple single point modifications in both the peptidic unit and the NP-inspired moiety to yield a structurally diverse library based on the DINNN epitope for further study of the key interactions that modulate the iNOS–SPSB2 interaction.

Investigation of 17 PepNats, bearing the DINNN epitope for binding to human SPSB2, revealed binding affinities from the low nanomolar to the micromolar range, as measured by Surface Plasmon Resonance (SPR) (Table 1, entries 1–17).

In the *N*-methyl substituted fused di-pyrrolidine series (**D1**, **D8**–**D10**, **D12**, **D14**), variation of the N-methylated amino-acid next to the NP-inspired fragment and the amino acid side chain employed for aldehyde introduction clearly influences target affinity. PepNats **D10-major** (one carbon linker), **D9-major** (two carbon linker) and **D1-major** (four carbons) displayed comparable K_D values of 72 nM, 66 nM and 33 nM respectively (Table 1, entries 1, 2 and 4), whereas **D8-major** (three carbon linker) bound with nine-fold lower affinity than **D1-major** (Table 1, entries 3 and 4). For the N-methylated phenylalanine containing peptide sequence, the replacement of the methyl

substituent in the fused di-pyrrolidine NP-inspired fragment by a phenyl group resulted in seven-fold lower affinity with a K_D of 231 nM (PepNat **D2-major**; Table 1, entry 8). Variation of the N-methylated amino-acid next to the NP-inspired moiety from N-Me phenylalanine to N-Me leucine or N-Me valine was beneficial for the affinity (e.g. compare **D1-major** with **D12-major** or **D13-major**, and **D2-major** with **D18-major**; Table 1, entries 4, 6, 11 and 8, 14 respectively), and afforded cyclic PepNat SPSB2 binders with potency comparable to the 13-mer truncated *N*-terminal iNOS linear peptide[53] **22** (Table 1, entry 18) and with potency better than the linear DINNN epitope **23** (Table 1, entry 16). Both linear reference peptides were synthesized and tested in the SPR assay for comparison. The fused di-pyrrolidine-peptide macrocycle, **D18-major**, showed 14- and 28-fold improved binding affinity compared to the disulfide bridged analogue[9] **24**, or the related cyclic peptide **25,** which were synthesized independently as reference compounds and assessed in the SPR assay (Table 1, compare entry 13 with entries 20 and 21). To further demonstrate the ability of the NP-inspired unit to fine tune the conformation of the peptide epitope and improve the binding affinity to the hSPSB2 protein, the simple phenylmethanamine linker containing macrocycle **27** was synthesized. The synthesis employed the same precursor and imine cyclization as

described for the on resin imine/cycloaddition synthetic methodology described above, but followed by reductive amination instead of cycloaddition. The non-constrained macrocycle **27** bound hSPSB2 with 87 nM in affinity. For comparison the constrained PepNat **D18-major** which embodies sp^3 stereocenters in the NP-inspired unit binds hSPSB2 with 2 nM affinity (44-fold better affinity than **27**).

PepNats **D4-major** and **D7-major** embodying the four carbon linker and N-Me phenylalanine in combination with a pyrrolidine and a pyrrolidinyl-spirobarbiturate NP-inspired scaffolds respectively, bound with low nanomolar affinity (Table 1, entries 16 and 15). The pyrrolidinyl-spirobarbiturate NP containing PepNat **D7-major** showed 3.8 nM affinity for the hSPSB2 and resulted in 4-fold and 46-fold higher affinity compared to the disulfide bridged peptide[9] **24** or the ortho ether aromatic unit analogue[14] **26** respectively (compare Table 1, entry 12 with Table 1, entries 17, 19).

Table 1. Binding affinities of the cyclic DINNN-PepNats for the hSPSB2 protein determined by SPR

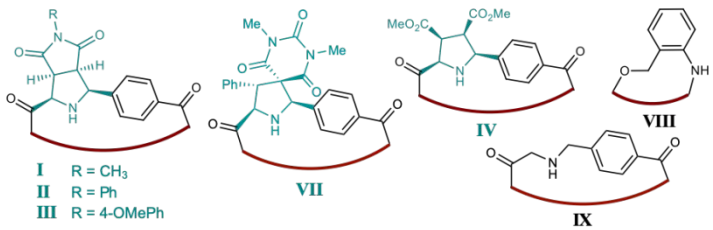

entry	compound	structure*	K_D (nM)†
1	**D10-major**	[I-**F**DINNNDap]G	72 ± 16
2	**D9-major**	[I-**F**DINNNDab]G	66 ± 8
3	**D8-major**	[I-**F**DINNNOrn]G	282 ± 93
4	**D1-major**	[I-**F**DINNNK]G	33 ± 15
5	**D15-major**	[I-**f**DINNNK]G	> 10000
6	**D12-major**	[I-**L**DINNNK]G	10 ± 4
7	**D12-minor**	[I-**L**DINNNK]G	127 ± 9
8	**D2-major**	[II-**F**DINNNK]G	231 ± 43
9	**D3-major**	[III-**F**DINNNK]G	309 ± 39
10	**D17-major**	[II-**F**DINNNDap]G	1080 ± 76
11	**D13-major**	[I-**V**DINNNK]G	15 ± 2
12	**D13-minor**	[I-**V**DINNNK]G	78 ± 19
13	**D18-major**	[II-**V**DINNNK]G	2.2 ± 0.3
14	**D18-minor**	[II-**V**DINNNK]G	139 ± 76
15	**D7-major**	[VII-**F**DINNNK]G	3.8 ± 0.5
16	**D4-major**	[IV-**F**DINNNK]G	18 ± 7
17	**D4-minor**	[IV-**F**DINNNK]G	> 10000
18	**22**[53]	Ac-KEEKDINNNVKKT	7.1 ± 1.5
19	**23**[9]	Ac-DINNN	237 ± 34
20	**24**[9]	[CVDINNNC]	16 ± 4
21	**25**[66]	[WDINNNβA]	79 ± 10
22	**26**[14]	[**VIII**-DINNN]	175 ± 6
23	**27**	[**IX**-**F**DINNNK]	87 ± 2

* [ ] indicates cyclic structure; Dap = Diaminopropanoic acid; Dab = Diaminobutanoic acid; Orn = Ornithine; Lower case letters indicate D-amino acids; bold residues are N-methylated. † K_D values are presented in nanomolar (nM) concentration as mean ± Standard Error of the Mean (SEM) of three independent experiments using Surface Plasmon Resonance (SPR) (for selected sensorgrams see Supplementary Figure S8).

Notably, the stereochemistry of the NP-inspired fragment seems to induce different conformational constraints on the loop epitope which translates into very different binding potency between the major vs. minor isomer. Thus, for PepNat **D4**, the major (2*R*, 3*S*, 4*R*, 5*S*) diastereomer showed nanomolar affinity for SPSB2 (K_D = 18 nM), while the minor (2*S*, 3*R*, 4*S*, 5*R*) diastereomer did not bind (Table 1, entries 16 and 17). This observation was also made for the *N*-methyl fused di-pyrrolidine PepNat **D13** and the *N*-phenyl fused di-pyrrolidine-DINNN macrocycle **D18** with a 5-fold and 63-fold loss of binding for the minor diastereomer respectively (Table 1, entries 11, 13 and 12, 14).

Further, it should be noted that linkers not incorporating stereogenic centers such as disulfide bridged compound **24**, ortho ether aromatic unit **VI** in peptidomimetic **26** and phenylmethanamine **VII** in cyclic peptidomimetic **27**, require separate and lengthy syntheses (for synthesis details, see Supplementary Information Section 3, E). These syntheses only afforded a single DINNN analogue that did not have improved affinity for the protein of interest, hSPSB2. Further, these corresponding macrocycles did not show increased potency compared to the full length linear precursor or other previously reported cyclic DINNN containing peptides. In contrast, the flexible and rapid synthesis

methodology reported here, readily yielded diverse PepNats bearing the same DINNN epitope and afforded novel more potent binders for the hSPSB2 protein.

RFF/Rff-PepNats selectively target different melanocortin receptor isoforms

Achieving selectivity within a protein family frequently represents a major challenge. As a second application of PepNats for hot loop mimicry, we therefore targeted the melanocortin (MC) receptor family, since structure and amino acid sequence similarity between the five melanocortin receptor (MC1–5R) isoforms renders the design of selective peptide or peptidomimetic ligands particularly challenging. The human AGouti Related Protein (AGRP) is an antagonist of MC receptors, and consequently this PPI can serve as a starting point for novel modulators. Binding analysis of the AGRP *C*-terminal domain employing cyclic disulfide-bridged peptides identified the Y[CRFFNAFC]Y sequence as hot loop responsible for agonistic activity at the mouse MC1R with low selectivity.[67, 68, 69] Within this loop, the RFF sequence (hAGRP$^{111\text{-}113}$) represents hot spot residues responsible for receptor binding[70] and replacement of the phenylalanines by their D-analogues modulates selectivity and MC1R agonistic activity.[10]

Synthesis and investigation of the reported cyclic disulfide-bridged peptides[68] Y[CRFFNAFC]Y **28** and Y[CRffNAFC]Y **29** (Figure 6a) as references, revealed that peptide **28** displayed micromolar affinity for the human MC receptors with apparent

selectivity for MC4R. Agonistic activity for the human MC1R was improved by incorporation of D-phenylalanine in cyclic peptide Y[CRffNAFC]Y **29** (Figure 6a). However, the binding selectivity profile was reduced.

To investigate whether combination of adjustable NP-inspired scaffolds with the AGRP$^{109\text{-}118}$ hot loop would yield selective ligands with distinct peptide conformations, binding and functional activity of 33 cyclic PepNats were determined (Supplementary Table S5). Indeed, variation of the amino acid structure around the key hot spots (RFF or Rff) and the NP-inspired moiety yielded selective compounds with sub-micromolar binding affinity. Introduction of different NP-inspired scaffolds into a given hot loop resulted in different selectivity profiles which could not be obtained with simple unstructured linkers.

a

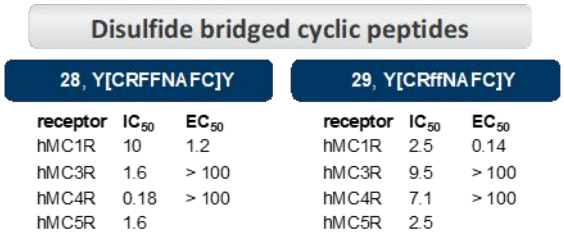

b

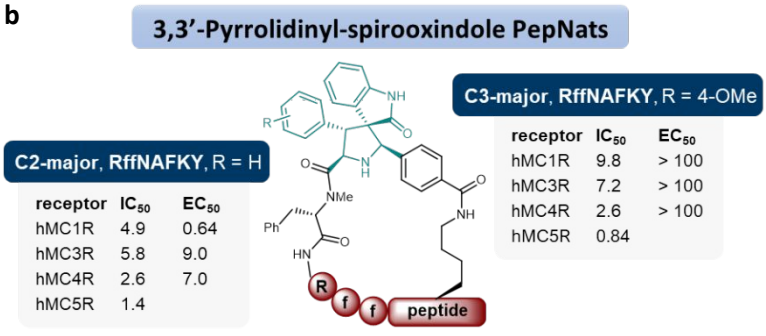

c

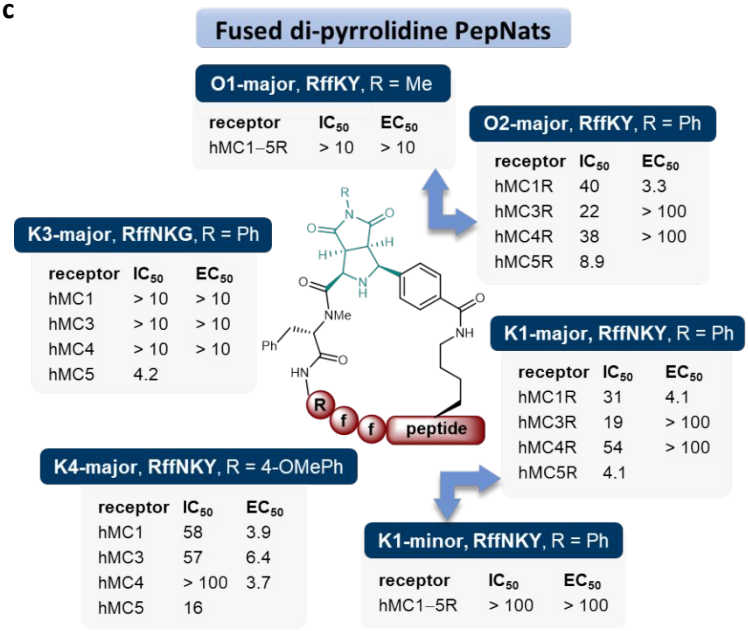

Figure 6. Binding and functional activity of the hAGRP epitope based PepNats to the melanocortin (MC) receptors. IC_{50} (competitive binding affinity) and EC_{50} (cAMP assay) are reported in micromolar (μM) as means of at least three independent experiments. For a complete list of binding and functional activity including SEM see Supplementary Table S5. For selected binding and functional curves see Supplementary Figure S9. Peptide sequences are represented as single capital letter code. Lower case letters indicate D-amino acids. (a) Binding affinity and functional activity for the disulfide-bridged cyclic peptides; [ ] indicates cyclic structures. (b) Binding affinity and functional activity reported for selected examples of the 3,3'-pyrrolidinyl-spirooxindole PepNats. (c) Binding affinity and functional activity reported for selected examples of the fused di-pyrrolidine PepNats.

3,3'-Pyrrolidinyl-spirooxindole PepNats **C2** and **C3** displayed affinities in the low micromolar to sub-micromolar range (Figure 6b, Supplementary Table S5). PepNat **C3-major** exhibited high affinity for the MC5R (IC_{50} = 0.84 μM) with 10-fold selectivity against MC1R, MC3R and MC4R.

For the 29 PepNats containing the fused di-pyrrolidine moiety, i.e. **B1**–**B3**, **C4**, **F1**, **F2**, **G1**, **J1**–**J3**, **K1**–**K5**, **N1**–**N3**, **O1** and **O2**, the $AGRP^{109-118}$ hot loop was truncated stepwise to the tripeptide hot spot (Supplementary Table S5). In general, in this group, compounds with the *N*-phenyl substituted fused di-pyrrolidine displayed the highest affinity for the MC receptors (Figure 6c). Thus, *N*-phenyl substituted PepNat **O2-major** which contains only the truncated Rff hot spot bound to the four receptors and showed MC1R agonistic activity, while *N*-methyl analogue **O1-major** was essentially inactive. Further functionalization of the phenyl ring by a methoxy group in PepNat **K4-major** resulted in decrease of affinity compared to the unsubstituted phenyl group analogue, **K3-major** (Figure 6c). PepNats **N1**–**N3** and **O2-major** are the smallest known macrocycles inspired by the AGRP, which bind to the MC receptors with selectivity for the MC5R and partial agonistic activity at the MC1R.

As observed for the DINNN PepNats, variation of the absolute configuration of the NP-inspired fragments correlated with affinity. For the *N*-phenyl substituted fused di-pyrrolidines, the major (2*R*, 3*S*, 4*R*, 5*S*) diastereomers displayed in general higher activity and a better receptor subtype selectivity profile than the minor (2*R*, 3*S*, 4*R*, 5*S*)-configured PepNats (Figure 6c). For example, **K1-major** bound the MC5R (IC_{50} = 4.1 μM) with 7-, 5- and 13-fold selectivity compared to MC1R, MC3R and MC4R respectively and is a partial MC1R agonist. On the contrary, the minor diastereomer **K1-minor** did not bind to any of the receptors. Analysis of the NMR spectra of PepNat **K1-major** and **K1-minor** in deuterated methanol at room temperature, revealed that these differences in affinity and selectivity for the diastereomers correlate with two distinct preferred major conformations in solution (Supplementary Figure S3b and Supplementary Information, Section 5). This further corresponds to the PepNat conformation in solution described for the model PepNat **H1** as described above (Figure 5, Supporting Information).

▪Conclusion

Protein loops display a diverse set of structures and often position their termini in spatial proximity. Notably, such loops frequently mediate PPIs ("hot loops")[4, 5] and adopt various conformations which may not readily be mirrored by means of available mimicking strategies. We describe a new principle for the design and synthesis of a hot loop mimicking modality, termed PepNats. In these peptide-NP-inspired mixed modalities, NP-inspired structures are incorporated into macrocyclic peptides derived from hot loop sequences. By analogy to known macrocyclic natural products, like the jasplakinolides and the chondramides, which contain peptidic and non-peptidic structures, in these hybrid modalities the peptide conformation can be installed or adjusted through the structure, notably the stereogenic character, of the non-peptidic units which themselves may primarily modulate but not directly mediate binding to the target proteins. Efficient PepNat synthesis is required to meet the demands of peptide and stereoselective NP synthesis, both preferably on solid support.

We provide proof-of-principle by the design, synthesis and analysis of macrocyclic PepNat collections representing hot loop epitopes. PepNat synthesis on solid support was successfully achieved by integration of established solid phase peptide synthesis with organic synthesis methods usually applied in asymmetric synthesis in solution.

This includes assembly of the peptide chains, subsequent macrocyclization *via* imine formation and final stereoselective 1,3-dipolar cycloaddition of azomethine ylides generated *in situ* from the Schiff bases by deprotonation. The synthesis method is rapid and flexible, has wide scope and efficiently delivers the desired PepNats in viable overall yields and purity suitable for developing structure-activity relationships. In particular, it does not require pre-synthesis of special building blocks to be included in the solid phase synthesis, but rather the NP-inspired structure-determining fragments are built up on resin as integral part of a flexible SPPS technique. This opens up an opportunity for fully automated syntheses of focused compound libraries. Structural and conformational analysis revealed that the major and minor diastereomers adopt very different conformations in solution as depicted by NMR-MD analysis simulation and the difference in binding affinity for the targeted protein.

PepNats embodying and derived from the DINNN hot loop characteristic for inducible nitric oxide synthase (iNOS) are novel and potent ligands of the hSPSB2 adaptor protein in the E3 ubiquitin ligase complex that ubiquitinates iNOS. PepNats derived from the RFF hot spot sequence in human agouti-related protein (AGRP) delivered selective ligands and agonists for the MC receptors. In both cases, the absolute

configuration of the PepNats correlates with binding affinity for the protein of interest. For the melanocortin receptor, the flexible modification of the NP-inspired unit in the PepNats yielded a modulable selectivity profile for the different receptor types while maintaining the same epitope inspired from the AGRP sequence. Taken together, these results demonstrate that the combination of NP-inspired scaffolds with a "Ω hot loop" yielded PepNats with conformationally constrained biologically relevant structure.

▪ ASSOCIATED CONTENT

Supplementary Figures and Tables; detailed materials and methods; full experimental procedures and analytical data for all the PepNats; as well as the conformational analysis are available in the Supporting Information. This supporting information is available free of charge *via* the Internet at http://pubs.acs.org.

▪ AUTHOR INFORMATION

Corresponding Authors

*stephanie.gueret@astrazeneca.com

*herbert.waldmann@mpi-dortmund.mpg.de

Present Address

†Integrated Drug Discovery, Sanofi-Aventis Deutschland GmbH, Frankfurt am Main, Germany.

Notes

The authors declare no competing interests.

▪ ACKNOWLEDGEMENT

The authors acknowledge Tomas Leek for helping with the analytical analysis of the diastereomers and Wolf-Gerald Hiller at the NMR facility of the TU Dortmund. Carola Wassvik and Maria Saxin are acknowledged for initial assistance with the NMR conformational analysis. The authors thank Laura-Marie Zimmermann and Marie Perrin for contribution in side projects related to PepNats. Finally, the authors acknowledge Andrey Antonchick and Laurent Knerr for fruitful discussion.

▪ REFERENCES

1. Arkin, M. R.; Tang, Y.; Wells, J. A., Small-molecule inhibitors of protein-protein interactions: progressing toward the reality. *Chem. Biol.* **2014,** *21* (9), 1102-14.

2. Scott, D. E.; Bayly, A. R.; Abell, C.; Skidmore, J., Small molecules, big targets: drug discovery faces the protein-protein interaction challenge. *Nat. Rev. Drug Discov.* **2016,** *15* (8), 533-50.

3. Valeur, E.; Gueret, S. M.; Adihou, H.; Gopalakrishnan, R.; Lemurell, M.; Waldmann, H.; Grossmann, T. N.; Plowright, A. T., New Modalities for Challenging Targets in Drug Discovery. *Angew. Chem. Int. Ed.* **2017,** *56* (35), 10294-10323.

4. Gavenonis, J.; Sheneman, B. A.; Siegert, T. R.; Eshelman, M. R.; Kritzer, J. A., Comprehensive analysis of loops at protein-protein interfaces for macrocycle design. *Nat. Chem. Biol.* **2014,** *10* (9), 716-22.

5. Siegert, T. R.; Bird, M. J.; Makwana, K. M.; Kritzer, J. A., Analysis of Loops that Mediate Protein-Protein Interactions and Translation into Submicromolar Inhibitors. *J. Am. Chem. Soc.* **2016,** *138* (39), 12876-12884.

6. Villar, E. A.; Beglov, D.; Chennamadhavuni, S.; Porco, J. A., Jr.; Kozakov, D.; Vajda, S.; Whitty, A., How proteins bind macrocycles. *Nat. Chem. Biol.* **2014,** *10* (9), 723-31.

7. Harjani, J. R.; Yap, B. K.; Leung, E. W.; Lucke, A.; Nicholson, S. E.; Scanlon, M. J.; Chalmers, D. K.; Thompson, P. E.; Norton, R. S.; Baell, J. B., Design, Synthesis, and Characterization of Cyclic Peptidomimetics of the Inducible Nitric Oxide Synthase Binding Epitope That Disrupt the Protein-Protein Interaction Involving SPRY Domain-Containing Suppressor of Cytokine Signaling Box Protein (SPSB) 2 and Inducible Nitric Oxide Synthase. *J. Med. Chem.* **2016,** *59* (12), 5799-809.

8. Owens, A. E.; de Paola, I.; Hansen, W. A.; Liu, Y. W.; Khare, S. D.; Fasan, R., Design and Evolution of a Macrocyclic Peptide Inhibitor of the Sonic Hedgehog/Patched Interaction. *J. Am. Chem. Soc.* **2017,** *139* (36), 12559-12568.

9. Di Maro, S.; Trotta, A. M.; Brancaccio, D.; Di Leva, F. S.; La Pietra, V.; Ieranò, C.; Napolitano, M.; Portella, L.; D'Alterio, C.; Siciliano, R. A.; Sementa, D.; Tomassi, S.; Carotenuto, A.; Novellino, E.; Scala, S.; Marinelli, L., Exploring the N-Terminal Region of C-X-C Motif Chemokine 12 (CXCL12): Identification of Plasma-Stable Cyclic Peptides As Novel, Potent C-X-C Chemokine Receptor Type 4 (CXCR4) Antagonists. *J. Med. Chem.* **2016,** *59* (18), 8369-8380.

10. Joseph, C. G.; Wang, X. S.; Scott, J. W.; Bauzo, R. M.; Xiang, Z.; Richards, N. G.; Haskell-Luevano, C., Stereochemical studies of the monocyclic agouti-related protein (103-122) Arg-Phe-Phe residues: conversion of a melanocortin-4 receptor antagonist into an agonist and results in the discovery of a potent and selective melanocortin-1 agonist. *J. Med. Chem.* **2004,** *47* (27), 6702-6710.

11. Yap, B. K.; Leung, E. W.; Yagi, H.; Galea, C. A.; Chhabra, S.; Chalmers, D. K.; Nicholson, S. E.; Thompson, P. E.; Norton, R. S., A potent cyclic peptide targeting SPSB2 protein as a potential anti-infective agent. *J. Med. Chem.* **2014,** *57* (16), 7006-7015.

12. Kale, S. S.; Villequey, C.; Kong, X. D.; Zorzi, A.; Deyle, K.; Heinis, C., Cyclization of peptides with two chemical bridges affords large scaffold diversities. *Nat Chem* **2018,** *10* (7), 715-723.

13. Reguera, L.; Rivera, D. G., Multicomponent Reaction Toolbox for Peptide Macrocyclization and Stapling. *Chem. Rev.* **2019,** *Article ASAP*.

14. Reguera, L.; Rivera, D. G., Multicomponent Reaction Toolbox for Peptide Macrocyclization and Stapling. *Chem. Rev.* **2019,** *119* (17), 9836-9860.

15. Hili, R.; Rai, V.; Yudin, A. K., Macrocyclization of linear peptides enabled by amphoteric molecules. *J. Am. Chem. Soc.* **2010,** *132* (9), 2889-91.

16. Frost, J. R.; Scully, C. C.; Yudin, A. K., Oxadiazole grafts in peptide macrocycles. *Nat. Chem.* **2016,** *8* (12), 1105-1111.

17. Smolyar, I. V.; Yudin, A. K.; Nenajdenko, V. G., Heteroaryl Rings in Peptide Macrocycles. *Chem. Rev.* **2019**.

18. Nitsche, C.; Onagi, H.; Quek, J. P.; Otting, G.; Luo, D.; Huber, T., Biocompatible Macrocyclization between Cysteine and 2-Cyanopyridine Generates Stable Peptide Inhibitors. *Org. Lett.* **2019,** *21* (12), 4709-4712.

19. Seigal, B. A.; Connors, W. H.; Fraley, A.; Borzilleri, R. M.; Carter, P. H.; Emanuel, S. L.; Fargnoli, J.; Kim, K.; Lei, M.; Naglich, J. G.; Pokross, M. E.; Posy, S. L.; Shen, H.; Surti, N.; Talbott, R.; Zhang, Y.; Terrett, N. K., The discovery of macrocyclic XIAP antagonists from a DNA-programmed chemistry library, and their optimization to give lead compounds with in vivo antitumor activity. *J. Med. Chem.* **2015,** *58* (6), 2855-61.

20. Mendive-Tapia, L.; Preciado, S.; Garcia, J.; Ramon, R.; Kielland, N.; Albericio, F.; Lavilla, R., New peptide architectures through C-H activation stapling between tryptophan-phenylalanine/tyrosine residues. *Nat. Commun.* **2015,** *6*, 7160.

21. Li, B.; Li, X.; Han, B.; Chen, Z.; Zhang, X.; He, G.; Chen, G., Construction of Natural-Product-Like Cyclophane-Braced Peptide Macrocycles via sp(3) C-H Arylation. *J. Am. Chem. Soc.* **2019,** *141* (23), 9401-9407.

22. Lee, H.; Sylvester, K.; Derbyshire, E. R.; Hong, J., Synthesis and Analysis of Natural-Product-Like Macrocycles by Tandem Oxidation/Oxa-Conjugate Addition Reactions. *Chemistry (Easton)* **2019,** *25* (26), 6500-6504.

23. Guo, Z.; Hong, S. Y.; Wang, J.; Rehan, S.; Liu, W.; Peng, H.; Das, M.; Li, W.; Bhat, S.; Peiffer, B.; Ullman, B. R.; Tse, C. M.; Tarmakova, Z.; Schiene-Fischer, C.; Fischer, G.; Coe, I.; Paavilainen, V. O.; Sun, Z.; Liu, J. O., Rapamycin-inspired macrocycles with new target specificity. *Nat. Chem.* **2018,** *11*, 254-263.

24. Allen, S. E.; Dokholyan, N. V.; Bowers, A. A., Dynamic Docking of Conformationally Constrained Macrocycles: Methods and Applications. *ACS Chem. Biol.* **2016,** *11* (1), 10-24.

25. Tannert, R.; Milroy, L. G.; Ellinger, B.; Hu, T. S.; Arndt, H. D.; Waldmann, H., Synthesis and structure-activity correlation of natural-product inspired cyclodepsipeptides stabilizing F-actin. *J. Am. Chem. Soc.* **2010,** *132* (9), 3063-77.

26. Feliu, L.; Planas, M., Cyclic Peptides Containing Biaryl and Biaryl Ether Linkages. *Int. J. Pep. Res. Ther.* **2005,** *11* (1), 53-97.

27. He, Y. P.; Tan, H.; Arve, L.; Baumann, S.; Waldmann, H.; Arndt, H. D., Biphenomycin B and derivatives: total synthesis and translation inhibition. *Chem. Asian J.* **2011,** *6* (6), 1546-56.

28. Tan, Y. X.; Romesberg, F. E., Latent antibiotics and the potential of the arylomycins for broad-spectrum antibacterial activity. *Med. Chem. Commun.* **2012,** *3*, 916-925.

29. Appavoo, S. D.; Kaji, T.; Frost, J. R.; Scully, C. C. G.; Yudin, A. K., Development of Endocyclic Control Elements for Peptide Macrocycles. *J. Am. Chem. Soc.* **2018,** *140* (28), 8763-8770.

30. Marimganti, S.; Yasmeen, S.; Fischer, D.; Maier, M. E., Synthesis of jasplakinolide analogues containing a novel omega-amino acid. *Chem. Eur. J.* **2005,** *11* (22), 6687-6700.

31. Roberts, T. C.; Smith, P. A.; Cirz, R. T.; Romesberg, F. E., Structural and initial biological analysis of synthetic arylomycin A2. *J. Am. Chem. Soc.* **2007,** *129* (51), 15830-15838.

32. Stevers, L. M.; Sijbesma, E.; Botta, M.; MacKintosh, C.; Obsil, T.; Landrieu, I.; Cau, Y.; Wilson, A. J.; Karawajczyk, A.; Eickhoff, J.; Davis, J.; Hann, M.; O'Mahony, G.; Doveston, R. G.; Brunsveld, L.; Ottmann, C., Modulators of 14-3-3 Protein-Protein Interactions. *J. Med. Chem.* **2018,** *61* (9), 3755-3778.

33. Over, B.; Wetzel, S.; Grutter, C.; Nakai, Y.; Renner, S.; Rauh, D.; Waldmann, H., Natural-product-derived fragments for fragment-based ligand discovery. *Nat. Chem.* **2013,** *5* (1), 21-8.

34. Brun, O.; Elduque, X.; Pedroso, E.; Grandas, A., On-Resin Conjugation of Diene-Polyamides and Maleimides via Diels-Alder Cycloaddition. *J. Org. Chem.* **2015,** *80* (12), 6093-6101.

35. Cironi, P.; Alvarez, M.; Albericio, F., Solid-phase chemistry in the total synthesis of non-peptidic natural products. *Mini-Rev. Med. Chem.* **2006,** *6* (1), 11-25.

36. Lessmann, T.; Waldmann, H., Enantioselective synthesis on the solid phase. *Chem. Commun.* **2006,** (32), 3380-9.

37. Riveira, M. J.; Diez, C. M.; Mischne, M. P.; Mata, E. G., [2 + 2 + 2]-Cycloaddition Reactions Using Immobilized Alkynes. A Proof of Concept for an Integral Use of the Outcoming Products in Solid-Phase Synthetic Methodologies. *J. Org. Chem.* **2018,** *83* (17), 10001-10014.

38. Senaiar, R. S.; Teske, J. A.; Young, D. D.; Deiters, A., Synthesis of indanones via solid-supported [2+2+2] cyclotrimerization. *J. Org. Chem.* **2007,** *72* (20), 7801-7804.

39. Malins, L. R.; deGruyter, J. N.; Robbins, K. J.; Scola, P. M.; Eastgate, M. D.; Ghadiri, M. R.; Baran, P. S., Peptide Macrocyclization Inspired by Non-Ribosomal Imine Natural Products. *J. Am. Chem. Soc.* **2017,** *139* (14), 5233-5241.

40. Guéret, S. M.; Meier, P.; Roth, H. J., Cyclic carbo-isosteric depsipeptides and peptides as a novel class of peptidomimetics. *Org. Lett.* **2014,** *16* (5), 1502-5.

41. Adrio, J.; Carretero, J. C., Novel dipolarophiles and dipoles in the metal-catalyzed enantioselective 1,3-dipolar cycloaddition of azomethine ylides. *Chem. Commun.* **2011,** *47* (24), 6784-94.

42. Narayan, R.; Potowski, M.; Jia, Z. J.; Antonchick, A. P.; Waldmann, H., Catalytic enantioselective 1,3-dipolar cycloadditions of azomethine ylides for biology-oriented synthesis. *Acc. Chem. Res.* **2014,** *47* (4), 1296-1310.

43. Stanley, L. M.; Sibi, M. P., Enantioselective copper-catalyzed 1,3-dipolar cycloadditions. *Chem. Rev.* **2008,** *108* (8), 2887-902.

44. Dadiboyena, S.; Nefzi, A., Solid Phase Synthesis of Isoxazole and Isoxazoline-carboxamides via [2+3]-Dipolar Cycloaddition Using Resin-bound Alkynes or Alkenes. *Tetrahedron Lett.* **2012,** *53* (16), 2096-2099.

45. Fuci, N.; Doi, T.; Cao, B.; Kahn, M.; Takahashi, T., The Solid-Phase Parallel Synthesis of -Strand Mimetic Templates via 1,3-Dipolar Cycloaddition with Resin-bound Vinylsulfone. *SynLett* **2002,** *2*, 285-289.

46. Harju, K.; Vesterinen, J.; Yli-Kauhaluoma, J., Solid-phase synthesis of amino acid derived N-unsubstituted pyrazoles via sydnones. *Org. Lett.* **2009,** *11* (10), 2219-2221.

47. Bochis, R. J.; Fisher, M. H., The structure of Palasonin. *Tetrahedron Lett.* **1968,** *16*, 1971-1974.

48. Ericson, M. D.; Lensing, C. J.; Fleming, K. A.; Schlasner, K. N.; Doering, S. R.; Haskell-Luevano, C., Bench-top to clinical therapies: A review of melanocortin ligands from 1954 to 2016. *Biochim. Biophys. Acta, Mol. Basis Dis.* **2017,** *1863*, 2414-2435.

49. Goldfarb, D. S. Method for altering the lifespan of eukaryotic organisms. US 2009/0163545 A1, 2009.

50. Plunkett, A. O., Pyrrole, pyrrolidine, pyridine, piperidine, and azepine alkaloids. *Nat. Prod. Rep.* **1994,** *11* (6), 581-90.

51. Galliford, C. V.; Scheidt, K. A., Pyrrolidinyl-spirooxindole natural products as inspirations for the development of potential therapeutic agents. *Angew. Chem. Int. Ed.* **2007,** *46* (46), 8748-58.

52. Kaur, M.; Singh, M.; Chadha, N.; Silakari, O., Oxindole: A chemical prism carrying plethora of therapeutic benefits. *Eur. J. Med. Chem.* **2016,** *123*, 858-894.

53. Marti, C.; Carreira, Erick M., Construction of Spiro[pyrrolidine-3,3′-oxindoles] − Recent Applications to the Synthesis of Oxindole Alkaloids. *Eur. J. Org. Chem.* **2003,** *2003* (12), 2209-2219.

54. Hunter, A. C.; Schlitzer, S. C.; Stevens, J. C.; Almutwalli, B.; Sharma, I., A Convergent Approach to Diverse Spiroethers through Stereoselective Trapping of Rhodium Carbenoids with Gold-Activated Alkynols. *J. Org. Chem.* **2018,** *83* (5), 2744-2752.

55. Liu, H.; Liu, Y.; Yuan, C.; Wang, G. P.; Zhu, S. F.; Wu, Y.; Wang, B.; Sun, Z.; Xiao, Y.; Zhou, Q. L.; Guo, H., Enantioselective Synthesis of Spirobarbiturate-Cyclohexenes through Phosphine-Catalyzed Asymmetric [4 + 2] Annulation of Barbiturate-Derived Alkenes with Allenoates. *Org. Lett.* **2016,** *18* (6), 1302-5.

56. Lomlim, L.; Einsiedel, J.; Heinemann, F. W.; Meyer, K.; Gmeiner, P., Proline derived spirobarbiturates as highly effective beta-turn mimetics incorporating polar and functionalizable constraint elements. *J. Org. Chem.* **2008,** *73* (9), 3608-11.

57. Cabrera, S.; Gomez Arrayas, R.; Carretero, J. C., Highly enantioselective copper(I)-fesulphos-catalyzed 1,3-dipolar cycloaddition of azomethine ylides. *J. Am. Chem. Soc.* **2005,** *127* (47), 16394-5.

58. Aguilar, A.; Sun, W.; Liu, L.; Lu, J.; McEachern, D.; Bernard, D.; Deschamps, J. R.; Wang, S., Design of chemically stable, potent, and efficacious MDM2 inhibitors that exploit the retro-mannich ring-opening-cyclization reaction mechanism in spiro-oxindoles. *J. Med. Chem.* **2014,** *57* (24), 10486-98.

59. Hosseinzadeh, P.; Bhardwaj, G.; Mulligan, V. K.; Shortridge, M. D.; Craven, T. W.; Pardo-Avila, F.; Rettie, S. A.; Kim, D. E.; Silva, D. A.; Ibrahim, Y. M.; Webb, I. K.; Cort, J. R.; Adkins, J. N.; Varani, G.; Baker, D., Comprehensive computational design of ordered peptide macrocycles. *Science* **2017,** *358* (6369), 1461-1466.

60. Yudin, A. K., Macrocycles: lessons from the distant past, recent developments, and future directions. *Chem. Sci.* **2015,** *6* (1), 30-49.

61. Appavoo, S. D.; Kaji, T.; Frost, J. R.; Scully, C. C. G.; Yudin, A. K., Development of Endocyclic Control Elements for Peptide Macrocycles. *J. Am. Chem. Soc.* **2018,** *140* (28), 8763-8770.

62. Appavoo, S. D.; Huh, S.; Diaz, D. B.; Yudin, A. K., Conformational Control of Macrocycles by Remote Structural Modification. *Chem. Rev.* **2019,** *119* (17), 9724-9752.

63. Woo, J. S.; Suh, H. Y.; Park, S. Y.; Oh, B. H., Structural basis for protein recognition by B30.2/SPRY domains. *Mol. Cell* **2006,** *24* (6), 967-76.

64. Filippakopoulos, P.; Low, A.; Sharpe, T. D.; Uppenberg, J.; Yao, S.; Kuang, Z.; Savitsky, P.; Lewis, R. S.; Nicholson, S. E.; Norton, R. S.; Bullock, A. N., Structural basis for Par-4 recognition by the SPRY domain- and SOCS box-containing proteins SPSB1, SPSB2, and SPSB4. *J. Mol. Biol.* **2010,** *401* (3), 389-402.

65. Kuang, Z.; Lewis, R. S.; Curtis, J. M.; Zhan, Y.; Saunders, B. M.; Babon, J. J.; Kolesnik, T. B.; Low, A.; Masters, S. L.; Willson, T. A.; Kedzierski, L.; Yao, S.; Handman, E.; Norton, R. S.; Nicholson, S. E., The SPRY domain-containing SOCS box protein SPSB2 targets iNOS for proteasomal degradation. *J. Cell Biol.* **2010,** *190* (1), 129-41.

66. Sadek, M. M.; Barlow, N.; Leung, E. W. W.; Williams-Noonan, B. J.; Yap, B. K.; Shariff, F. M.; Caradoc-Davies, T. T.; Nicholson, S. E.; Chalmers, D. K.; Thompson, P. E.; Law, R. H. P.; Norton, R. S., A Cyclic Peptide Inhibitor of the iNOS-SPSB Protein-Protein Interaction as a Potential Anti-Infective Agent. *ACS Chem. Biol.* **2018,** *13* (10), 2930-2938.

67. Ericson, M. D.; Wilczynski, A.; Sorensen, N. B.; Xiang, Z.; Haskell-Luevano, C., Discovery of a beta-Hairpin Octapeptide, c[Pro-Arg-Phe-Phe-Dap-Ala-Phe-DPro], Mimetic of Agouti-Related Protein(87-132) [AGRP(87-132)] with Equipotent Mouse Melanocortin-4 Receptor (mMC4R) Antagonist Pharmacology. *J. Med. Chem.* **2015,** *58* (11), 4638-47.

68. Haskell-Luevano, C.; Monck, E. K.; Wan, Y. P.; Schentrup, A. M., The agouti-related protein decapeptide (Yc[CRFFNAFC]Y) possesses agonist activity at the murine melanocortin-1 receptor. *Peptides* **2000,** *21* (5), 683-9.

69. Tota, M. R.; Smith, T. S.; Mao, C.; MacNeil, T.; Mosley, R. T.; Van der Ploeg, L. H.; Fong, T. M., Molecular interaction of Agouti protein and Agouti-related protein with human melanocortin receptors. *Biochemistry* **1999,** *38* (3), 897-904.

70. McNulty, J. C.; Thompson, D. A.; Bolin, K. A.; Wilken, J.; Barsh, G. S.; Millhauser, G. L., High-resolution NMR structure of the chemically-synthesized melanocortin receptor binding domain AGRP(87-132) of the agouti-related protein. *Biochemistry* **2001,** *40* (51), 15520-7.

For Table of Contents Only